Final Technical Report

GeoSoilEnviroCARS: A National Resource for Earth, Planetary, Soil and Environmental Science Research at the Advanced Photon Source

DE-FG02-94ER14466
(University of Chicago)

Project Period: August 15, 1994 to August 14, 2018

Submitted by

Steve Sutton and Mark Rivers

April 2019

Table of Contents

A Executive Summary 3
B Project Overview 4
C Sector Status 4
C.1 Undulator Beamline (13ID) 6
C.2 Bending Magnet Beamline (13BM) 7
D Science Program Overview 8
D.1 Reactions at Mineral-Water Interfaces 8
D.2 Flow Dynamics of Fluids and Solids 8
D.3 Biogeochemistry 8
D.4 Chemistry of Magmas and their associated Hydrothermal Fluids 9
D.5 High Pressure Mineral Physics and Chemistry 9
D.6 Non-crystalline and Nano-crystalline Materials at High Pressure 9
D.7 Cosmochemical Studies of Extraterrestrial Materials 10
E General User Program 10
F Management Structure 10
G Outreach/Expansion Initiatives 11
H Science Highlights 13
H.1 Mineral-Water Interfaces 13
H.1.1 Structure of the Hydrated α-Al_2O_3 (0001) Surface 13
H.1.2 Oxidative Corrosion of the UO_2 (001) Surface by Nonclassical Diffusion 13
H.1.3 Hydration Structure of the Barite (001)−Water Interface 14
H.1.4 Dynamic Stabilization of Metal Oxide–Water Interfaces 14
H.1.5 Mineral–Water Interface Structure of Xenotime (YPO_4) {100} 14
H.1.6 Structure and Reactivity of the Calcite-Water Interface 15
H.1.7 Simultaneous U(VI) Sorption Complexes and U(IV) Nanoprecipitates on Magnetite 15
H.1.8 Tetravalent Thorium Sorption on Muscovite 16
H.1.9 Surface-Mediated Formation of Pu(IV) Nanoparticles: Muscovite-Electrolyte Interface 16
H.1.10 Competitive Sorption on Polyacrylic Acid-Coated Hydrated Aluminum-Oxide Surfaces 17
H.2 Flow Dynamics 17
H.2.1 Enhancing Residual Trapping of Supercritical CO_2 Via Cyclic Injections 17
H.2.2 Ion Diffusion Within Water Films in Unsaturated Porous Media 17
H.2.3 Nanoscale Brine Film Thicknesses: Silica Surfaces under CO_2 Sequestration Conditions 18
H.2.4 Crude Oil Distribution and Removal from Homogeneous Porous Media 18
H.2.5 Pore-Scale Observations of Supercritical CO_2 Drainage in Sandstone 19
H.2.6 Transport of U(VI) through Sediments Amended with Phosphate 19
H.3 Biogeochemistry 20
H.3.1 Tetravalent Uranium in Calcite 20
H.3.2 Impacts of Detrital on Contaminant Dynamics in a Coal Mine AMD Treatment System 20
H.3.3 Redox Transformations of As and Se at the Surfaces of Ferric Nontronites 20
H.3.4 Oxidation and Mobilization of Metallic Antimony in Aqueous Systems 21
H.3.5 Cr(VI) Treatment by Zero-Valent Iron 21
H.3.6 Microbial Enhanced Oil Recovery in Fractional-Wet Systems 22
H.3.7 Sulfur-Mediated Electron Shuttling During Bacterial Iron Reduction 22
H.3.8 Uranium in Oxidized Wetland Sediment from the Savannah River Site 22

A Executive Summary

This project partially supported GeoSoilEnviroCARS (GSECARS), a national user facility for frontier research in the earth sciences using synchrotron radiation at the Advanced Photon Source (APS), Argonne National Laboratory, and the foremost synchrotron-based facility dedicated to serving the needs of the geoscience community. The DOE-supported research advanced our knowledge of the composition, structure and properties of earth materials. Frontier experiments were conducted in research areas including mineral-water interface reactions, biogeochemical cycling, flow dynamics of fluids and solids, and projects relevant to applied programs. Examples of these experimental topics include oxygen diffusion in energy-relevant materials, interface structural studies of materials undergoing electrochemical reactions, biogeochemical reactions in aquifers and deep storage reservoirs, reactions in zero-valent iron reactive barriers, and uranium.

This project used synchrotron x-ray beams produced by the APS DOE User Facility. All principal synchrotron-based analytical techniques in demand by earth scientists were available at GSECARS. The most DOE-relevant techniques included powder, single crystal and interface diffraction; inelastic x-ray scattering; x-ray absorption fine structure spectroscopy; x-ray fluorescence microprobe analysis; and microtomography. A proposal-based, peer-reviewed system implemented by the APS was the basis for beam time allocation at GSECARS. A recently-completed canted undulator upgrade (funded separately) doubled the available undulator beam time and provided new capabilities, notably microprobe access to lower energies (down to the sulfur K edge) and enhanced flux at high energy.

The research had broad impact on society because it addressed quality-of-life issues such as carbon sequestration, environmental remediation, and properties of nanomaterials. GSECARS provided a research environment where users received expert assistance in planning and conducting experiments and in analyzing data. This collaborative mode of operation, which allowed GSECARS to be accessible to students and synchrotron radiation novices, required a staff of highly qualified beamline scientists and technical personnel. GSECARS developed advanced hardware and software that benefitted many accelerator facilities worldwide.

B Project Overview

GeoSoilEnviroCARS (GSECARS) is a national user facility dedicated to frontier research in the earth, environmental and planetary sciences. The research conducted at this facility is advancing our knowledge of the composition, structure and properties of earth materials, the processes they control and the processes that produce them. Most principal synchrotron-based analytical techniques in demand by these scientists are available for use by the entire community: (1) high-pressure/high-temperature powder diffraction and spectroscopy using the diamond anvil cell (DAC); (2) high-pressure/high-temperature powder diffraction and imaging using the large-volume press; (3) micro X-ray absorption fine structure spectroscopy; (4) micro X-ray fluorescence and powder micro-diffraction mapping; (5) microtomography; (6) high-pressure/high-temperature single crystal diffraction in the DAC (7) high-pressure/high-temperature total scattering in the DAC and PE cell. (8) powder and interface diffraction.

GSECARS has been funded cooperatively by the Department of Energy Geosciences program (and other BES initiatives e.g. Midscale Instrumentation) and by the National Science Foundation (Earth Sciences Instrumentation and Facilities Program) since 1994. The DE-FG02-94ER14466 awards to the University of Chicago have, in coordination with other funding sources, supported the following tasks (among others):

- Design, procurement, fabrication, assembly, testing, commissioning and operation of beamline components including X-ray mirror systems, experimental stations, beam transport, vacuum systems, radiation shielding, and safety systems.
- Design, procurement, fabrication, assembly, testing, commissioning and operation of analytical instrumentation including sample manipulation systems, detectors, electronics, high pressure devices, specialized analytical equipment such as X-ray microprobe, General Purpose Diffractometer, and Computed Tomography Apparatus.
- Operation and maintenance of the GSECARS sector instrumentation and associated computing systems.
- Conduct technical development projects aimed at advancing the capabilities of the sector.
- Manage a general user program for geoscience applications at the sector
- Collaborate on user experiments (experiment design, sample selection and preparation, analytical conditions, data collection, etc.) to maximize success rate.
- Analysis, interpretation and archiving of all generated datasets
- Production of manuscripts for publication in peer-reviewed journals

C Sector Status

The sector consists of canted undulator beamlines (13ID), a split bending magnet beamline (13BM), and three support laboratories. Each beamline consists of a first optics enclosure (13ID-A and 13BM-A), second optics enclosure (13ID-B and 13BM-B), and experimental stations (13ID-C, 13ID-D, 13ID-E, 13BM-C, and 13BM-D). Four of the five experimental stations operate simultaneously: 13BM-C, 13BM-D, 13ID-E, and 13ID-C or 13ID-D.

GSECARS Sector Layout – Advanced Photon Source Sector 13

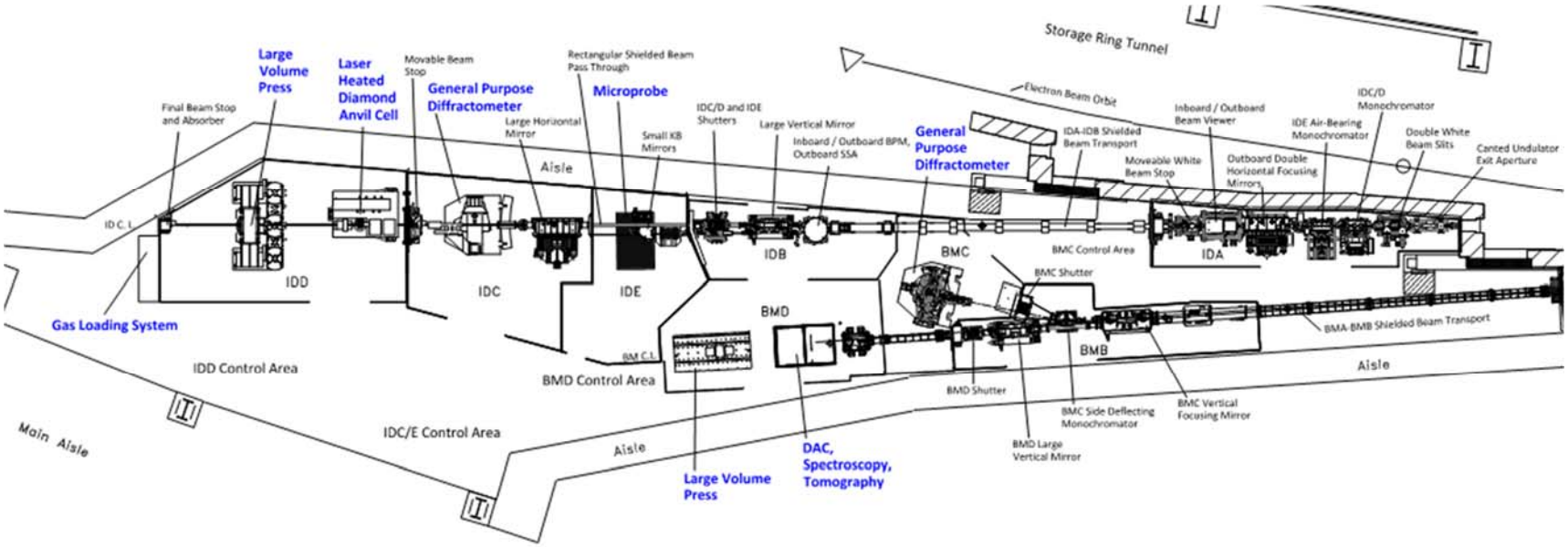

The primary instrumentation and techniques available in each station are summarized below:

C.1 Undulator Beamline (13ID)

- Station 13ID-A (1st Optical Enclosure): Primary beamline slits, two cryogenic Si (111 & 311) monochromators, diagnostic tanks, horizontal deflecting and focusing mirrors (13ID-E), white beam power limiting aperture. (13ID-C/D)
- Station 13ID-B (2nd Optical Enclosure): Vertical focusing mirror (13ID-C/D), secondary source aperture (13ID-E), diagnostic tank with BPM's for 13ID-E and 13ID-C/D, inboard and outboard branch safety shutters
- Station 13ID-C (1st Experimental Station): Horizontal focusing mirror (13ID-C/D), General Purpose Diffractometer (crystal truncation rod, X-ray standing waves, reflectivity, grazing incidence XRF, grazing incidence XAFS, inelastic X-ray scattering, microcrystallography)
- Station 13ID-D (2nd Experimental Station): Laser Heated Diamond Anvil Cell Diffractometer (angular dispersive micro-diffraction, emission spectroscopy); 1000-ton Multi-anvil Press (energy dispersive diffraction, angular dispersive diffraction, radiography)
- Station 13ID-E (3rd Experimental Station): X-ray Microprobe (microXRF, microXAFS, microXRD, fluorescence microtomography)

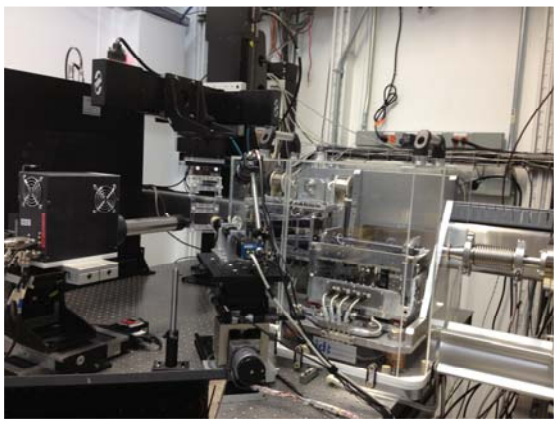

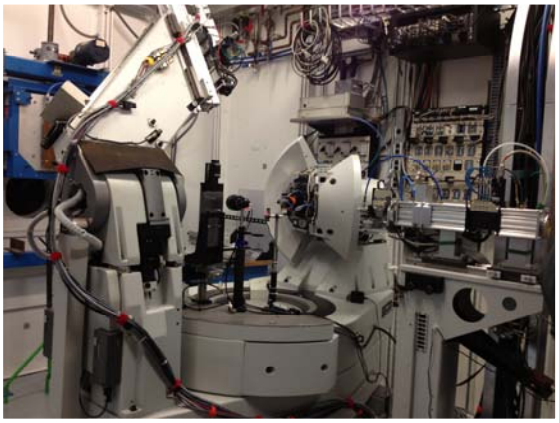

X-ray microprobe in station 13ID-E (left) is used for microXRF, microXAFS, microXRD, fluorescence microtomography to study the chemical and mineralogical compositions of heterogeneous earth materials at high spatial resolution**. General Purpose Diffractometer in station 13ID-C (right)** is used for CTR, standing waves and other surface sensitive techniques to study interfaces and surfaces.

C.2 Bending Magnet Beamline (13BM)

- Station 13BM-A (1st Optical Enclosure): Primary beamline slits, water-cooled Si (111) monochromator (13BM-D)
- Station 13BM-B (2nd Optical Enclosure): Vertical focusing mirror (13BM-D), vertical focusing mirror (13BM-C); horizontal focusing Si (111 & 311) monochromator (13BM-C), shutters (13BM-D and 13BM-C)
- Station 13BM-C (Side Experimental Station): General Purpose Diffractometer (powder and single crystal diffraction in the DAC, crystal truncation rod, X-ray standing waves, reflectivity, powder diffraction, microcrystallography,)
- Station 13BM-D (End Experimental Station): Externally Heated Diamond Anvil Cell Diffractometer (angular dispersive micro-diffraction, Brillouin and Raman spectroscopy); Microtomography Apparatus (transmission and differential absorption computed microtomography); 250-ton Multi-anvil Press (energy dispersive diffraction, angular dispersive diffraction, radiography, high-pressure tomography)

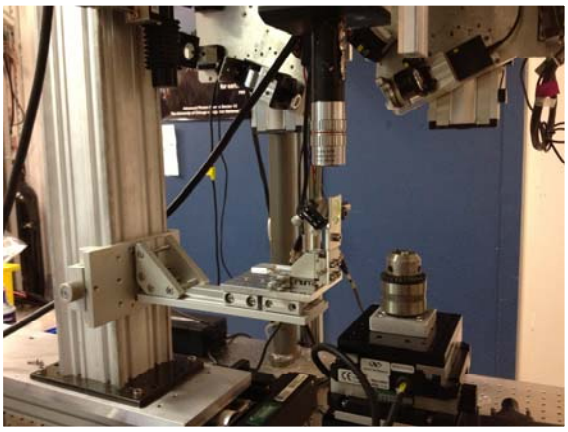

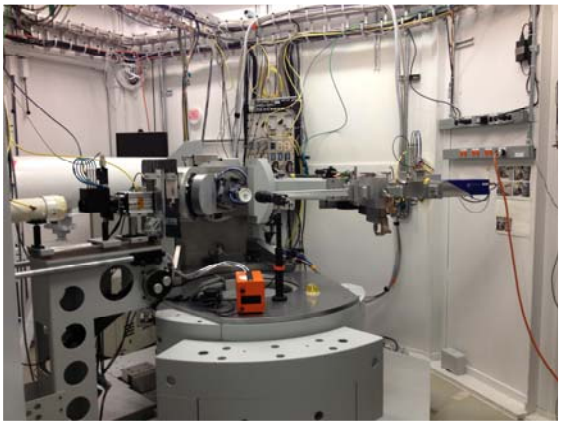

Microtomography apparatus in station 13BM-D (left) is used to study the 3D structure and flow behavior of earth materials and associated fluids with high spatial resolution. **General Purpose Diffractometer in station 13BM-C (right)** is used for crystal truncation rod, X-ray standing waves, reflectivity, powder diffraction, microcrystallography.

D Science Program Overview

A wide range of research is being undertaken covering topics including processes at work in the Earth's crust that control the transport and bio-availability of toxic species; the chemistry, nature, and dynamics of Earth's interior; and the evolution of our solar system revealed through the study of extraterrestrial materials. The majority of this research can be divided into the following categories arranged roughly in order of relevance to the DOE-Geosciences mission:

D.1 Reactions at Mineral-Water Interfaces

Chemical interactions at interfaces between solids and aqueous solutions often dominate the fate and transport of trace elements and pollutants within the Earth's hydrosphere and are largely responsible for the trace element composition of the oceans. As such, the overall composition and speciation of an aquatic system are strongly influenced by processes such as: (i) the adsorption of dissolved species on the surfaces of mineral phases (including nanoparticles), fine-grained amorphous materials, organic and microbial materials, and inorganic and/or organic films coating mineral surfaces; (ii) the incorporation of dissolved species within phases precipitated from solution; (iii) release of chemical species to solution through dissolution or desorption; and (iv) mobilization or flocculation of nanoparticles. The development of a fundamental understanding of these processes requires detailed experimental studies of the structure, composition, and chemical mechanisms at solid-aqueous solution interfaces. A number of complementary surface-sensitive techniques are currently in place at GSECARS including; (1) crystal truncation rod diffraction and grazing-angle reflectivity for the analysis of surface and interface structure; (2) X-ray absorption fine structure and grazing-incidence absorption spectroscopy to probe the local structure and oxidation state of surface-bound species; and (3) X-ray standing wave fluorescence-yield measurements for the determination of the position and distribution of surface and interfacial species. The GSECARS General Purpose Diffractometers allow a combination of these techniques to be applied on samples under *in situ* conditions (i.e., in the presence of bulk solution or controlled atmosphere).

D.2 Flow Dynamics of Fluids and Solids

Many processes in the earth's surface are controlled by the microscale interaction of water and air with the solid phase (soils, sediments, rock) in pore spaces within the subsurface. The distribution in time and space of fluids in pores ultimately controls subsurface flow and transport processes relevant to groundwater resource management and remediation as well as oil and gas exploration and recovery. Many of the mechanisms operating at the microscale can be observed through the measurement of relevant physical parameters (e.g. fluid phase content and distribution, pore size distribution, permeability, porosity) using computed microtomography. In addition, the flow of solids is important in understanding earthquake propagation.

D.3 Biogeochemistry

Improving the accuracy of contaminant transport models is one of the biggest challenges facing environmental geochemists. Bacteria are ubiquitous in surface waters and in the subsurface, even to depths of several kilometers. These microbes have an extremely high affinity to adsorb aqueous metal cations, and the ability to mediate redox reactions, potentially dominating the speciation of the metals in the environment. An important aspect of the research at GSECARS is to improve our understanding of the molecular-scale processes that control contaminant-microbe adsorption and redox reactions, and the effect of these processes on contaminant transport. The

GSECARS microprobe provides instrumentation to biogeochemists for measuring redox mediated changes in chemistry (from the S K-edge through to the Cd K-edge) at appropriate length scales, both in natural samples and within environmentally-controlled experimental cells.

D.4 Chemistry of Magmas and their associated Hydrothermal Fluids

Microfocused X-ray absorption fine structure techniques allow for direct measurement of the speciation of redox sensitive elements (eg. Fe, V, Cr, Eu, Ti, S, etc.) in magmatic minerals and glasses. Since oxygen fugacity (fO_2) plays a vital role in determining the stability and composition of crystallizing phases, the oxidation state of multivalent elements, and the composition and stability of fluid and volatile phases in a magma, such direct measurement of elemental speciation and valence allows researchers to then quantitatively constrain the redox conditions for magmas derived by the melting of planetary mantles. This is critical to our understanding of the genesis and differentiation of magmas, associated ore deposits and for modeling the evolution of planetary interiors. These XAFS methods are also applied in studying the hydrothermal fluids associated with magmatic systems. Hot fluids within the Earth are important conduits for chemical transport. For example, ore-deposits such as porphyry Cu and epithermal Au(Cu) form from metals transported as complex ions in hydrothermal solutions. To understand the formation of these deposits, it is necessary to determine the metal complexes, and their stability, as a function of variables such as temperature and fluid composition. The GSECARS microprobe is well-suited for such studies using X-ray absorption spectroscopic techniques on individual fluid inclusions, both natural and synthetic.

D.5 High Pressure Mineral Physics and Chemistry

The primary goal of high-pressure mineral physics research is to provide a laboratory basis for understanding the state and dynamics of the Earth's deep interior. Together, the diamond anvil cell (DAC) and large volume press (LVP) apparatus provide a powerful resource for studies of the structures and properties of minerals under the precise pressure and temperature conditions at all depths within the Earth. The GSECARS high pressure instrumentation is utilized for a wide range of experiments related to the composition of the Earth's mantle and core and the processes at work in the deep Earth including equations of state and phase relations, element partitioning, accurate structural determinations, elasticity, rheology, kinetics of phase transformations, and chemical reactions at extreme conditions.

D.6 Non-crystalline and Nano-crystalline Materials at High Pressure

Critical for modeling processes of planetary differentiation is a detailed knowledge of the rheological properties of silicate melts and the melting properties of Earth materials at conditions reaching those in the deep mantle. The GSECARS LVPs allow direct measurement of melt viscosities at high pressures using real-time X-ray radiography to monitor the fall of dense marker spheres through molten silicate melt. Melting temperatures at high pressure can be inferred in the DAC through observations of diffuse scattering and the disappearance of crystalline diffraction peaks. Liquid and amorphous structure measurements are performed using the total scattering technique in both the DAC and a Paris-Edinburgh press using Soller slits and a new Pilatus 300K CdTe detector. The grain size dependence of phase transitions in nano-crystalline materials can also be investigated in the DAC.

D.7 Cosmochemical Studies of Extraterrestrial Materials

Clues to the origin and evolution of our Solar System and other cosmological bodies are locked within extraterrestrial materials available for laboratory study including lunar samples returned by the Apollo program; meteorites from the Moon, Mars and asteroids; interplanetary dust particles collected in the stratosphere; comet particles collected by the Stardust spacecraft; and solar wind collected by the Genesis spacecraft. Synchrotron-based techniques, primarily X-ray microprobe, tomography, microXAFS and X-ray standing waves, allow us to define the chemical states of these samples and obtain insight into the properties of their parent bodies.

E General User Program

The GSECARS research program has been and continues to be organized and managed as a User Program in full operation since Fall 1998. Essentially 100% of the available user operations beam time is allocated through the proposal-based, APS General User Program. The APS Beamtime Allocation Committee allocates 25% of the available time (a standard requirement of all sectors) and GSECARS allocates the remaining 75%. These allocations are based foremost on the ratings of peer-review panels consisting of external experts. Research at GSECARS has resulted in over 2,100 publications in the APS database including 216 PhD and Masters theses.

The GSECARS sector continues to be oversubscribed and the oversubscription rate continues to increase. In the last, 3-month scheduling cycle of this grant period (2018-2), the sector received 183 beam time proposals for a total of 1,382 shifts (196 shifts available for each of the four GSECARS beamlines). The oversubscription for 2018 ranged from 1.1 (13BM-D) to 2.9 (13ID-C/D) where the oversubscription factor is defined to be the ratio of the number of days requested by users (Sector 13 first choice) to the number of days available to users. We handle this oversubscription by limiting the number of days each experiment receives, rejecting experiments, and referring experiments to other suitable synchrotron facilities. The challenge has been to balance the desire to give beam time to as many highly rated proposals as possible while providing sufficient beam time to each experiment to accomplish the intended goals. The proposal success rate continues to be near 60%. GSECARS is typically utilized by ~ 600 unique users per year (i.e., users with multiple allocated experiments in the period were only counted once), users who came from all over the world (~60% from the US) and were mostly affiliated with universities (~75%). About 60% of the GSECARS users are students at universities and colleges. Thus, the level of student participation at GSECARS is very high.

GSECARS staff work with prospective users to help them submit beam time proposals, to prepare samples before they arrive, to collect their data, and to analyze the data and prepare it for publication after they leave the facility. Publications resulting from work at GSECARS frequently include one or more GSECARS beamline scientists as co-authors.

F Management Structure

GSECARS is part of the Center for Advanced Radiation Sources (CARS) at the University of Chicago. CARS (Mark Rivers, Executive Director) operates sectors 13, 14, and 15 at the APS. GSECARS management consists of Co-Project Managers: Mark Rivers and Stephen Sutton, and six Technical Groups organized around the six principal techniques in the sector. Each of these groups has a senior GSECARS staff member as a leader as shown below:

- Diamond Anvil Cell: Vitali Prakapenka (lead; Research Professor), Sergey Tkachev (Beamline Scientist)
- Large-Volume Press: Yanbin Wang (lead, Research Professor), Tony Yu (Beamline Scientist)
- Microtomography: Mark Rivers (lead, Research Professor)
- X-ray Absorption Fine Structure Spectroscopy: Matt Newville (lead, Research Associate Professor), Tony Lanzirotti (Research Associate Professor)
- X-ray Diffraction and Scattering: Peter Eng (lead, Research Professor), Joanne Stubbs (Research Associate Professor)
- X-ray Fluorescence Microprobe: Stephen Sutton (lead, Research Professor)

These individuals have the responsibility to lead the development of science, instrumentation and user community in their particular area. In addition, they work closely with users to ensure the success of experiments (experiment design, experiment conduct, data analysis, etc.) and receive input from them on potential new technical directions. This management configuration has worked successfully throughout the history of GSECARS.

G Outreach/Expansion Initiatives

GeoSoilEnviroCARS operates as a national research resource for the entire earth, planetary, soil and environmental science communities. GSECARS uses a team approach, where lead individuals (scientists, engineers and technicians) from GSECARS work together with instrument companies and machine shops to design and build the complex array of components that go into a synchrotron beamline. During this process, we are able to welcome students at all levels— high school, undergraduate, graduate and post graduate— into our laboratory giving them the opportunity to learn about X-ray science and instrumentation as well as to be involved in hands-on activities in which they can experiment at building and testing instruments.

The proposal-based beam time allocation system facilitates the use of this technology by experts and novices alike. Training provided by the experienced GSECARS staff results in direct knowledge transfer to advance the quality of the nation's research infrastructure and to enhance the educational experience of students. Students trained under this program come from educational institutions across the nation and around the world, including the participation of underrepresented groups. GSECARS and its staff have a history of conducting workshops to instruct qualified individuals in the theoretical and practical aspects of synchrotron radiation techniques in use at the APS. We also host programs to introduce underrepresented minorities, women, and young students to synchrotron research. Recent examples of such activities by GSECARS include:

- Organized (with Miami University) XAFS Mini Workshop (2015)
- Organized a workshop at GSECARS (with ENS Paris) on applications of acoustic emission in synchrotron-based deformation experiments (2016)
- Co-organized a mini workshop at St. Louis Univ. on applications of seismological methods in acoustic experiments (2018)
- Participation in the NSF REU Program. The Research Experiences for Undergraduates (REU) program supports active research participation by undergraduate students in any of the areas of research funded by the National Science Foundation. REU projects involve students in meaningful ways in ongoing research programs or in research projects specifically designed for the REU program. (2015, 2017)

- Participation in the DOE INCREASE Workshop (Interdisciplinary Consortium for Research and Educational Access in Science and Engineering). INCREASE is a consortium of universities whose mission is to promote research and education in Minority-Serving Institutions, especially as regards increasing their utilization of national user facilities, thereby increasing the numbers of women and those from historically underrepresented groups who pursue science and engineering careers. (2015)
- Participation each year in the APS/IIT XAFS School (Matt Newville, guest instructor)
- Participation each year in the ANL Science Careers in Search of Women event.
- Participation each year in the ANL Introduce a Girl to Engineering Day event.
- Hosted a workshop on Acoustic Emission, which is a technique available at GSECARS in the multi-anvil presses (2016)
- Hosted Exemplary Student Research Program (ESRP) where local high school students conduct hands-on research and present posters at the APS User Meeting (2016., 2018)
- Participation in the APS/SNS X-ray/Neutron School with hands-on labs (2015, 2016)
- Helped sponsor the 2018 Workshop of the IUCr Commission on High Pressure. The purpose of the 2018 workshop was to bring together researchers who apply tools of extreme-conditions crystallography to different disciplines of science.
- Co-hosted a hands-on workshop dedicated to demonstrating the techniques and future developments of micro-manipulator using the Axis Pro Micromanipulation System. (2018)

H Science Highlights

Summarized here are representative studies with their associated publications to highlight the science accomplished at GSECARS. The emphasis is on recent work most relevant to the DOE-Geosciences program. The complete list of GSECARS publications, including hyperlinks to the actual journal articles, is archived in the APS Publication Database and can be accessed at:

https://beam.aps.anl.gov/pls/apsweb/pub_v2_0006.sector_query_all?i_sector_id=28

To search the GSECARS publication listing of over 2,100 entries, go to

https://beam.aps.anl.gov/pls/apsweb/pub_v2_0006.review_start_page

and choose "13 GSECARS" under "Sectors involved in work". Additional Science Highlights can be found in the previous Progress Reports for these awards.

H.1 Mineral-Water Interfaces

H.1.1 Structure of the Hydrated α-Al_2O_3 (0001) Surface

Publication: P. Eng, T.P. Trainor, G.E. Brown, Jr., G.A. Waychunas, S.R. Sutton, M.L. Rivers (2000) **Science** 288, 1029-1033.

The physical and chemical properties of the hydrated α-Al_2O_3 (0001) surface are important for understanding the reactivity of natural and synthetic aluminum-containing oxides. The structure of this surface was determined in the presence of water vapor at 300 kelvin by crystal truncation rod diffraction at a third-generation synchrotron x-ray source. The fully hydrated surface is oxygen terminated, with a 53% contracted double Al layer directly below. The structure is an intermediate between α-Al_2O_3 and γ-$Al(OH)_3$, a fully hydroxylated form of alumina. A semiordered oxygen layer about 2.3 angstroms above the terminal oxygen layer is interpreted as adsorbed water. The clean α-Al_2O_3 (0001) surface, in contrast, is Al terminated and significantly relaxed relative to the bulk structure. These differences explain the different reactivities of the clean and hydroxylated surfaces.

H.1.2 Oxidative Corrosion of the UO_2 (001) Surface by Nonclassical Diffusion

Publication: Joanne E. Stubbs, Craig A. Biwer, Anne M. Chaka, Eugene S. Ilton, Yingge Du, John R. Bargar, Peter J. Eng (2017), **Langmuir** 33 (46), 13189-13196. DOI: 10.1021/acs.langmuir.7b02800

Uranium oxide is central to every stage of the nuclear fuel cycle, from mining through fuel fabrication and use, to waste disposal and environmental cleanup. Its chemical and mechanical stability are intricately linked to the concentration of interstitial O atoms within the structure and the oxidation state of U. We have previously shown that, during corrosion of the UO_2 (111) surface under either 1 atm of O_2 gas or oxygenated water at room temperature, oxygen interstitials diffuse into the substrate to form a superlattice with three-layer periodicity. In the current study, we used surface X-ray scattering to reveal the structure of the oxygen diffusion profile beneath the (001) surface. The first few layers below the surface oscillate strongly in their surface-normal lattice parameters, suggesting preferential interstitial occupation of every other layer below the surface, which is geometrically consistent with the interstitial network that forms below the oxidized (111) surface. Deeper layers are heavily contracted and indicate that the oxidation front penetrates ~52

Å below the (001) surface after 21 days of dry O_2 gas exposure at ambient pressure and temperature. X-ray photoelectron spectroscopy indicates U is present as U(IV), U(V), and U(VI).

H.1.3 Hydration Structure of the Barite (001)−Water Interface

Publication: Jacquelyn N. Bracco, Sang Soo Lee, Joanne E. Stubbs, Peter J. Eng, Frank Heberling, Paul Fenter, and Andrew G. Stack (2017) **J. Phys. Chem. C** 121 (22), 12236-12248.

The three-dimensional structure of the barite (001)−water interface was studied using in situ specular and nonspecular X-ray reflectivity (XR). Displacements of the barium and sulfate ions in the surface of a barite crystal and the interfacial water structure were defined in the analyses. The largest relaxations (0.13 Å lateral and 0.08 Å vertical) were observed for the barium and sulfate ions in the topmost unit cell layer, which diminished rapidly with depth. The best fit structure identified four distinct adsorbed species, which in comparison with molecular dynamics (MD) simulations reveals that they are associated with positions of adsorbed water, each of which coordinates one or two surface ions (either barium, sulfate, or both). These water molecules also adsorb in positions consistent with those of bariums and sulfates in the bulk crystal lattice. These results demonstrate the importance of combining high resolution XR with MD simulations to fully describe the atomic structure of the hydrated mineral surface. The agreement between the results indicates both the uniqueness of the structural model obtained from the XR analysis and the accuracy of the force field used in the simulations.

H.1.4 Dynamic Stabilization of Metal Oxide–Water Interfaces

Publication: Martin E. McBriarty, Guido Falk von Rudorff, Joanne E. Stubbs, Peter J. Eng, Jochen Blumberger, Kevin M. Rosso (2017) **J. Am. Chem. Soc.** 139 (7), 2581-2584. DOI: 10.1021/jacs.6b13096

The interaction of water with metal oxide surfaces plays a crucial role in the catalytic and geochemical behavior of metal oxides. In a vast majority of studies, the interfacial structure is assumed to arise from a relatively static lowest energy configuration of atoms, even at room temperature. Using hematite (α-Fe_2O_3) as a model oxide, we show through a direct comparison of in situ synchrotron X-ray scattering with density functional theory-based molecular dynamics simulations that the structure of the $(1\bar{1}02)$ termination is dynamically stabilized by picosecond water exchange. Simulations show frequent exchanges between terminal aquo groups and adsorbed water in locations and with partial residence times consistent with experimentally determined atomic sites and fractional occupancies. Frequent water exchange occurs even for an ultrathin adsorbed water film persisting on the surface under a dry atmosphere. The resulting time-averaged interfacial structure consists of a ridged lateral arrangement of adsorbed water molecules hydrogen bonded to terminal aquo groups. Surface pK_a prediction based on bond valence analysis suggests that water exchange will influence the proton-transfer reactions underlying the acid/base reactivity at the interface. Our findings provide important new insights for understanding complex interfacial chemical processes at metal oxide–water interfaces. .

H.1.5 Mineral–Water Interface Structure of Xenotime (YPO_4) {100}

Publication: Andrew G. Stack, Joanne E. Stubbs, Sriram G. Srinivasan, Santanu Roy, Vyacheslav S. Bryantsev, Peter J. Eng, Radu Custelcean, Alexander D. Gordon, Cole R. Hexel (2018) **J. Phys. Chem. C** 122 (35), 20232-20243. DOI: 10.1021/acs.jpcc.8b04015

Crystal truncation rod (CTR) measurements and density functional theory (DFT) calculations were performed to determine the atomic structure of the mineral–water interface of the {100}

surface of xenotime (nominally YPO_4). This mineral is important, because it incorporates a variety of rare earth elements (REEs) in its crystal structure. REEs are critical materials necessary for a variety of renewable and energy efficient technologies. Current beneficiation techniques are not highly selective for REE ore minerals, and large amounts go to waste; this is a first step toward designing more efficient beneficiation. Evidence is found for minor relaxation of the surface within the topmost monolayer with little or no relaxation in subsurface layers. Justification for ordered water at the interface is found, where water binds to surface cations and donates hydrogen bonds to surface phosphates. The average bond lengths between cations and oxygens on water are 228 pm in the best fit to the CTR data, versus 243 and 251 pm for the DFT. No agreement on water positions bound to surface phosphates is obtained. Overall, the findings suggest that ligands used in beneficiation with a single anionic headgroup, such as fatty acids, will have limited selectivity for xenotime relative to undesirable minerals.

H.1.6 Structure and Reactivity of the Calcite-Water Interface

Publication: Heberling, F., T. P. Trainor, J. Lutzenkirchen, P. Eng, M. A. Denecke, and D. Bosbach (2011) **J. Colloid Interf. Sci.** 354, 843-857.

The zetapotential of calcite in contact with aqueous solutions of varying composition is determined for pre-equilibrated suspensions by means of electrophoretic measurements and for non-equilibrium solutions by means of streaming potential measurements. Carbonate and calcium are identified as charge determining ions. Studies of the equilibrium solutions show a shift of isoelectric point with changing CO_2 partial pressure. Changes in pH have only a weak effect in non-equilibrium solutions. The surface structure of (1 0 4)-faces of single crystal calcite in contact to solutions corresponding to those of the zetapotential investigations is determined from surface diffraction measurements. The results reveal no direct indication of calcium or carbonate inner-sphere surface species. The surface ions are found to relax only slightly from their bulk positions; the most significant relaxation is a ~4° tilt of the surface carbonate ions towards the surface. Two ordered layers of water molecules are identified, the first at 2.35 ± 0.05 Å above surface calcium ions and the second layer at 3.24 ± 0.06 Å above the surface associated with surface carbonate ions. A Basic-Stern surface complexation model is developed to model observed zetapotentials, while only considering outer-sphere complexes of ions other than protons and hydroxide. The Basic-Stern SCM successfully reproduces the zetapotential data and gives reasonable values for the inner Helmholtz capacitance, which are in line with the Stern layer thickness estimated from surface diffraction results.

H.1.7 Simultaneous U(VI) Sorption Complexes and U(IV) Nanoprecipitates on Magnetite

Publication: Singer, D. M., S. M. Chatman, E. S. Ilton, K. M. Rosso, J. F. Banfield, and G. A. Waychunas (2012) **Environ. Sci. Technol.** 46, 3811-3820.

Sequestration of uranium (U) by magnetite is a potentially important sink for U in natural and contaminated environments. However, molecular-scale controls that favor U(VI) uptake including both adsorption of U(VI) and reduction to U(IV) by magnetite remain poorly understood, in particular, the role of U(VI)–CO_3–Ca complexes in inhibiting U(VI) reduction. To investigate U uptake pathways on magnetite as a function of U(VI) aqueous speciation, we performed batch sorption experiments on (111) surfaces of natural single crystals under a range of solution conditions (pH 5 and 10; 0.1 mM U(VI); 1 mM $NaNO_3$; and with or without 0.5 mM CO_3 and 0.1 mM Ca) and characterized surface-associated U using grazing incidence extended X-ray absorption fine structure spectroscopy (GI-EXAFS), grazing incidence X-ray diffraction (GI-

XRD), and scanning electron microscopy (SEM). In the absence of both carbonate ([CO_3]T, denoted here as CO3) and calcium (Ca), or in the presence of CO_3 only, coexisting adsorption of U(VI) surface species and reduction to U(IV) occurs at both pH 5 and 10. In the presence of both Ca and CO_3, only U(VI) adsorption (VI) occurs. When U reduction occurs, nanoparticulate UO_2 forms only within and adjacent to surface microtopographic features such as crystal boundaries and cracks. This result suggests that U reduction is limited to defect-rich surface regions. Further, at both pH 5 and 10 in the presence of both CO_3 and Ca, U(VI)–CO_3–Ca ternary surface species develop and U reduction is inhibited. These findings extend the range of conditions under which U(VI)–CO_3–Ca complexes inhibit U reduction.

H.1.8 Tetravalent Thorium Sorption on Muscovite

Publication: M. Schmidt, S.S. Lee, R.E. Wilson, L. Soderholm, and P. Fenter (2012) **Geochim. Cosmochim. Acta** 88, 66-76.

Adsorption of tetravalent thorium to the (0 0 1) basal surface of the phyllosilicate muscovite from an aqueous solution (1×10^{-4} mol/L Th(IV) in 1×10^{-1} mol/L NaCl, pH = 3.2) was studied by crystal truncation rod (CTR) and resonant anomalous X-ray reflectivity (RAXR) measurements. Th uptake to the muscovite surface from solutions with total Th concentrations $[Th]_{tot} = 1 \times 10^{-6}$–$4.88 \times 10^{-3}$ mol/L and 1×10^{-1} mol/L NaCl, pH = 3.2 was quantified by alpha-spectrometry. The uptake measurements showed that Th adsorption to the muscovite surface follows a Langmuir isotherm with an apparent adsorption constant $K_{app} = 2 \times 10^4$ L/mol up to $[Th]_{tot} = 1.02 \times 10^{-3}$ mol/L. The CTR and RAXR results identified one dominant Th species with a very broad distribution centered ~10 Å above the surface, in agreement with strongly hydrated extended outer sphere sorption. The findings indicate that the large energy of hydration ($\Delta G_{hyd} = -5815$ kJ/mol (Marcus, 1991)) for the small and highly-charged Th^{4+} cation is a controlling parameter in its surface speciation. The surface occupancy (0.4 Th per unit cell area, A_{UC}) measured by RAXR exceeds the expected level for surface charge compensation by tetravalent Th (0.25 Th/A_{UC}). However, the radiometric uptake measurements show smaller occupancies (0.21 Th/A_{UC}) after rinsing by deionized water, indicating a partial removability of sorbed thorium. Thorium oligomerization was observed at total Th concentrations $[Th]_{tot} \geq 2.0 \times 10^{-3}$ mol/L in presence of the surface, although solubility studies suggest that Th is soluble under these solution conditions.

H.1.9 Surface-Mediated Formation of Pu(IV) Nanoparticles: Muscovite-Electrolyte Interface

Publication: Moritz Schmidt, Sang Soo Lee, Richard E. Wilson, Karah E. Knope, Francesco Bellucci, Peter J. Eng, Joanne E. Stubbs, L. Soderholm, P. Fenter (2013) **Environ. Sci. Technol.** 47 (24), 14178-14184.

The formation of Pu(IV)-oxo-nanoparticles from Pu(III) solutions by a surface-enhanced redox/polymerization reaction at the muscovite (001) basal plane was discovered with a continuous increase in plutonium coverage observed *in situ* over several hours. The sorbed Pu extended >70 Å from the surface with a maximum concentration at 10.5 Å and a total coverage of >9 Pu atoms per unit cell area of muscovite (0.77 μg Pu/cm^2) (determined independently by *in situ* resonant anomalous X-ray reflectivity and by ex-situ alpha-spectrometry). The presence of discrete nanoparticles was confirmed by high resolution atomic force microscopy. The formation of these Pu(IV) nanoparticles from an otherwise stable Pu(III) solution can be explained by the combination of a highly concentrated interfacial Pu-ion species, the Pu(III)–Pu(IV) redox equilibrium, and the strong proclivity of tetravalent Pu to hydrolyze and form polymeric species.

These results are the first direct observation of such behavior of plutonium on a naturally occurring mineral, providing insights into understanding the environmental transport of plutonium and other contaminants capable of similar redox/polymerization reactions.

H.1.10 Competitive Sorption on Polyacrylic Acid-Coated Hydrated Aluminum-Oxide Surfaces

Publication: Yingge Wang, F. Marc Michel, Clement Levard, Yong Choi, Peter J. Eng, Gordon E. Brown, Jr. (2013) **Environ. Sci. Technol.** 47 (21), 12131-12139.

Natural organic matter (NOM) often forms coatings on minerals. Such coatings are expected to affect metal–ion sorption due to abundant sorption sites in NOM and potential modifications to mineral surfaces, but such effects are poorly understood in complex multicomponent systems. Using poly(acrylic acid) (PAA), a simplified analog of NOM containing only carboxylic groups, Pb(II) and Zn(II) partitioning between PAA coatings and α-Al_2O_3 (1–102) and (0001) surfaces was investigated using long-period X-ray standing wave-fluorescence yield spectroscopy. In the single-metal–ion systems, PAA was the dominant sink for Pb(II) and Zn(II) for α-Al_2O_3(1–102) (63% and 69%, respectively, at 0.5 μM metal ions and pH 6.0). In equi-molar mixed-Pb(II)–Zn(II) systems, partitioning of both ions onto α-Al_2O_3(1–102) decreased compared with the single-metal–ion systems; however, Zn(II) decreased Pb(II) sorption to a greater extent than vice versa, suggesting that Zn(II) outcompeted Pb(II) for α-Al_2O_3(1–102) sorption sites. In contrast, >99% of both metal ions sorbed to PAA when equi-molar Pb(II) and Zn(II) were added simultaneously to PAA/α-Al_2O_3(0001). PAA outcompeted both α-Al_2O_3 surfaces for metal sorption but did not alter their intrinsic order of reactivity. This study suggests that single-metal–ion sorption results cannot be used to predict multimetal–ion sorption at NOM/metal–oxide interfaces when NOM is dominated by carboxylic groups.

H.2 Flow Dynamics

H.2.1 Enhancing Residual Trapping of Supercritical CO_2 Via Cyclic Injections

Publication: A. L. Herring, L. Andersson, D. Wildenschild (2016) **Geophys. Res. Lett.** 43 (18), 9677-9685

Synchrotron X-ray tomographic imaging was used to investigate the pore-scale characteristics and residual trapping of supercritical CO_2 ($scCO_2$) over the course of multiple drainage-imbibition (D-I) cycles in Bentheimer sandstone cores. Capillary pressure measurements were paired with X-ray image-derived saturation and connectivity metrics which describe the extent of drainage and subsequent residual (end of imbibition) $scCO_2$ trapping. For the first D-I cycle, residual $scCO_2$ trapping is suppressed due to high imbibition capillary number (Ca ≈ 10^{-6}); however, residual $scCO_2$ trapping dramatically increases for subsequent D-I cycles carried out at the same Ca value. This behavior is not predicted by conventional multiphase trapping theory. The magnitude of $scCO_2$ trapping increase is hysteretic and depends on the relative extent of the sequential drainage processes. The hysteretic pore-scale behavior of the $scCO_2$-brine-sandstone system observed in this study suggests that cyclic multiphase flow could potentially be used to increase $scCO_2$ trapping for sequestration applications.

H.2.2 Ion Diffusion Within Water Films in Unsaturated Porous Media

Publication: T. K. Tokunaga, S. Finsterle, Y. Kim, J. Wan, A. Lanzirotti, M. Newville (2017) **Environ. Sci. Technol.** 51 (8), 4338-4346.

Diffusion is important in controlling local solute transport and reactions in unsaturated soils and geologic formations. Although it is commonly assumed that thinning of water films controls solute diffusion at low water contents, transport under these conditions is not well understood. These experiments conducted in quartz sands at low volumetric water contents (θ) were used to quantify ion diffusion within adsorbed films. At the lowest water contents, fixed relative humidities were employed to control water films at nm thicknesses. Diffusion profiles for Rb^+ and Br^- in unsaturated sand packs were measured with a synchrotron X-ray microprobe, and inverse modeling was used to determine effective diffusion coefficients, D_e, as low as $\sim 9 \times 10^{-15}$ m^2 s^{-1} at $\theta = 1.0 \times 10^{-4}$ m^3 m^{-3}, where the film thickness = 0.9 nm. Given that the diffusion coefficients (D_o) of Rb^+ and Br^- in bulk water (30 °C) are both $\sim 2.4 \times 10^{-9}$ m^2 s^{-1}, we found the impedance factor $f = D_e/(\theta D_o)$ is equal to 0.03 ± 0.02 at this very low saturation, in agreement with the predicted influence of interface tortuosity (τa) for diffusion along grain surfaces. Thus, reduced cross-sectional area (θ) and tortuosity largely accounted for the more than 5 orders of magnitude decrease in D_e relative to D_o as desaturation progressed down to nanoscale films.

H.2.3 Nanoscale Brine Film Thicknesses: Silica Surfaces under CO_2 Sequestration Conditions

Publication: Kim, T. W., T. K. Tokunaga, D. B. Shuman, S. R. Sutton, M. Newville, and A. Lanzirotti (2012) **Water Resour. Res.** 48, W09558-1-W09558-13.

In reservoirs used for geologic CO_2 sequestration, brine films remaining on mineral surfaces can influence flow, diffusion, and reactions. We have investigated how the capillary (disjoining) potential influences the thickness of a $KCsI_2$ brine film on both smooth and rough SiO_2 surfaces [root mean square roughness (R_{rms}), 1.6 and 330 nm, respectively], under confinement with supercritical (sc) CO_2. The thicknesses of brine films coating interior surfaces of SiO_2 windows in a high-pressure cell were determined through synchrotron X-ray fluorescence of two tracer ions (I^- and Cs^+) at 7.8 MPa and 40°C (representative of conditions at about 0.78 km below the land surface), with $scCO_2$ as the immiscible confining fluid. The measured area-averaged film thicknesses on the 330 nm R_{rms} silica surface ranged from 265 to 249 nm for capillary potentials measured within a narrow range from 0.18 to 3.7 kPa. Over this same range of potentials, film thicknesses measured on the smooth (1.6 nm R_{rms}) silica surface were about 2 nm, although equilibrium does not appear to have been achieved. The measured average brine film thicknesses were strongly controlled by surface roughness, with very weak variation in response to the fairly narrow range of tested capillary potentials.

H.2.4 Crude Oil Distribution and Removal from Homogeneous Porous Media

Publication: Jaydeep Ghosh, Geoffrey R. Tick (2013) **J. Contam. Hydrol.** 155, 20-30.

A pore-scale study was conducted to understand interfacial processes contributing to the removal of crude oils from a homogeneous porous medium during surfactant-induced remediation. Synchrotron X-ray microtomography (SXM) was used to obtain high-resolution three-dimensional images of the two-fluid-phase oil/water system, and quantify temporal changes in oil blob distribution, blob morphology, and blob surface area before and after sequential surfactant flooding events. The reduction of interfacial tension in conjunction with the sufficient increase in viscous forces as a result of surfactant flushing was most likely responsible for mobilization and recovery of the two lighter oil fractions. However, corresponding increases in viscous forces as a result of a reduction of interfacial tension were insufficient to initiate and maintain the displacement (recovery) of the heavy crude oil fraction during surfactant flushing. In contrast to the heavy oil system, changes in trapping number for the lighter fraction crude oils were sufficient

to initiate mobilization as a result of surfactant flushing. Both light and medium oil fractions showed an increase in the number of blobs and total blob surface area, and a reduction in the total volume after 2 pore volumes (PVs) of surfactant flooding. This increase in surface area was attributed to the change in blob morphology from spherical to more complex non-spherical ganglia shape characteristics. Moreover, the increase in the number of oil blobs from larger to smaller particles after surfactant flushing may have contributed to the greater cumulative oil surface area. Complete recovery of light and medium oil fractions resulted after 5 PVs of surfactant flooding, whereas the displacement efficiency of heavy-oil fraction was severely limited, even after extended periods of flushing. The results of these experiments demonstrate the utility of SXM for quantifying pore-scale interfacial characteristics for specific crude-oil-fraction/porous-medium systems, critical for understanding mobilization/removal relationships in which surfactant-enhanced remediation techniques will be most successful.

H.2.5 Pore-Scale Observations of Supercritical CO_2 Drainage in Sandstone

Publication: Anna L. Herring, Linnea Andersson, D.L. Newell, J.W. Carey, D. Wildenschild (2014) **Int. J. Greenh. Gas Con.** 25, 93-101.

This work utilized synchrotron-based x-ray computed microtomography (x-ray CMT) imaging to quantify the volume and topology of supercritical carbon dioxide ($scCO_2$) on a pore-scale basis throughout the primary drainage process of a 6 mm diameter Bentheimer sandstone core. Experiments were performed with brine and $scCO_2$ at 8.3 MPa (1200 psi) and 37.5 °C. Capillary pressure–saturation curves for the $scCO_2$-brine system were compared to the ambient air-brine system, and overlay one another when pressure is normalized by interfacial tension. Results were analyzed from images with a voxel resolution of 4.65 μm; image-based evidence demonstrated that $scCO_2$ invades the pore space in a capillary fingering regime at a mobility ratio $M = 0.03$ and capillary number $Ca = 10^{-8.6}$ to an end-of-drainage brine saturation of 9%. The data provide evidence of the applicability of previous two-dimensional micromodel studies and ambient condition experiments in predicting flow regimes occurring during $scCO_2$ injection.

H.2.6 Transport of U(VI) through Sediments Amended with Phosphate

Publication: Vrajesh S. Mehta, Fabien Maillot, Zheming Wang, Jeffrey G. Catalano, Daniel E. Giammar (2015) **Water Res.** 69, 307-317.

Phosphate amendments can be added to U(VI)-contaminated subsurface environments to promote *in situ*remediation. The primary objective of this study was to evaluate the impacts of phosphate addition on the transport of U(VI) through contaminated sediments. In batch experiments using sediments (<2 mm size fraction) from a site in Rifle, Colorado, U(VI) only weakly adsorbed due to the dominance of the aqueous speciation by Ca-U(VI)-carbonate complexes. Column experiments with these sediments were performed with flow rates that correspond to a groundwater velocity of 1.1 m/day. In the absence of phosphate, the sediments took up 1.68-1.98 μg U/g of sediments when the synthetic groundwater influent contained 4 μM U(VI). When U(VI)-free influents were then introduced with and without phosphate, substantially more uranium was retained within the column when phosphate was present in the influent. Sequential extractions of sediments from the columns revealed that uranium was uniformly distributed along the length of the columns and was primarily in forms that could be extracted by ion exchange and contact with a weak acid. Laser induced fluorescence spectroscopy (LIFS) analysis along with sequential extraction results suggest adsorption as the dominant uranium uptake mechanism. The response of dissolved uranium concentrations to stopped-flow

events and the comparison of experimental data with simulations from a simple reactive transport model indicated that uranium adsorption to and desorption from the sediments was not always at local equilibrium.

H.3 Biogeochemistry

H.3.1 Tetravalent Uranium in Calcite

Publication: N. C. Sturchio, M. R. Antonio, L. Soderholm, S. R. Sutton, J. C. Brannon (1998) **Science** 281, 971-973.

X-ray absorption spectroscopy and x-ray fluorescence microprobe studies of 35-million-year-old calcite from a Mississippi Valley–type zinc ore deposit indicate substitution of tetravalent uranium for divalent calcium. Thus, tetravalent uranium has a stable location in calcite deposited under reducing conditions. This result validates uranium-series dating methods (including uranium/lead dating) for ancient calcite and shows that calcite provides a sink for uranium in deep groundwater aquifers and anoxic lacustrine and marine basins.

H.3.2 Impacts of Detrital on Contaminant Dynamics in a Coal Mine AMD Treatment System

Publication: Liliana Lefticariu, Stephen R. Sutton, Kelly S. Bender, Mihai Lefticariu, Martin Pentrak, Joseph W. Stucki (2017) **Sci. Total Environ.** 575, 941-955.

Pollutants in acid mine drainage (AMD) are usually sequestered in neoformed nano- and micro-scale particles (nNP) through precipitation, co-precipitation, and sorption. Subsequent biogeochemical processes may control nNP stability and thus long-term contaminant immobilization. Mineralogical, chemical, and microbiological data collected from sediments accumulated over a six-year period in a coal-mine AMD treatment system were used to identify the pathways of contaminant dynamics. We present evidence that detrital nano- and micron-scale particles (dNP), composed mostly of clay minerals originating from the partial weathering of coal-mine waste, mediated biogeochemical processes that catalyzed AMD contaminant (1) immobilization by facilitating heterogeneous nucleation and growth of nNP in oxic zones, and (2) remobilization by promoting phase transformation and reductive dissolution of nNP in anoxic zones. The dNP were found to be relatively stable under acidic conditions and estimated a dNP content of ~ 0.1 g/L in the influent AMD. In the AMD sediments, the initial nNP precipitates were schwertmannite and poorly crystalline goethite, which transformed to well-crystallized goethite, the primary nNP repository. Subsequent reductive dissolution of nNP resulted in the remobilization of up to 98% of S and 95% of Fe accompanied by the formation of a compact dNP layer. Effective treatment of pollutants could be enhanced by better understanding the complex, dynamic role dNP play in mediating biogeochemical processes and contaminant dynamics at coal-mine impacted sites.

H.3.3 Redox Transformations of As and Se at the Surfaces of Ferric Nontronites

Publication: Anastasia G. Ilgen, Jessica N. Kruichak, Kateryna Artyushkova, Matt G. Newville, and Chengjun Sun (2017) **Environ. Sci. Technol.** 51 (19), 11105-11114.

Adsorption and redox transformations on clay mineral surfaces are prevalent in surface environments. We examined the redox reactivity of iron Fe(II)/Fe(III) associated with natural and synthetic ferric nontronites. Specifically, we assessed how Fe(II) residing in the octahedral sheets, or Fe(II) adsorbed at the edge sites alters redox activity of nontronites. To probe the redox activity we used arsenic (As) and selenium (Se). Activation of both synthetic and natural ferric nontronites

was observed following the introduction of Fe(II) into predominantly-Fe(III) octahedral sheets or through the adsorption of Fe(II) onto the mineral surface. The oxidation of As(III) to As(V) was observed via catalytic (oxic conditions) and, to a lesser degree, via direct (anoxic conditions) pathways. We provide experimental evidence for electron transfer from As(III) to Fe(III) at the natural and synthetic nontronite surfaces, and illustrate that only a fraction of structural Fe(III) is accessible for redox transformations. We show that As adsorbed onto natural and synthetic nontronites forms identical adsorption complexes, namely inner-sphere binuclear bidentate. We show that the formation of an inner-sphere adsorption complex may be a necessary step for the redox transformation via catalytic or direct oxidation pathways.

H.3.4 Oxidation and Mobilization of Metallic Antimony in Aqueous Systems

Publication: A.G. Ilgen, F. Majs, A.J. Barker, T.A. Douglas, T.P. Trainor (2014) **Geochim. Cosmochim. Acta** 132, 16-30.

Antimony (Sb) is a contaminant of concern that can be present in elevated concentrations in shooting range soils due to mobilization from spent lead/antimony bullets. Antimony in shooting range soils has been observed as either metallic Sb(0) or as Sb(V) immobilized by iron (hydr)oxides. The absence of Sb(III) in soils is indicative of rapid Sb(III) oxidation to Sb(V) under surface soil conditions. However, the major controls on antimony oxidation and mobility are poorly understood. To better understand these controls, multiple batch experiments were performed under oxic conditions to quantify the oxidation and dissolution of antimony in systems where Sb(0) is oxidized to Sb(III) and further to Sb(V). The partially oxidized Sb(0) powders were characterized by means of extended X-ray absorption fine structure (EXAFS) spectroscopy and powder X-ray diffraction (XRD). The observed oxidation of Sb(0) to Sb(III) and mobilization to solution is rapid: after 5–15 min of reaction the aqueous antimony concentration reached 50–600 μM. The amount of dissolved antimony and the rate of Sb(III) oxidation to Sb(V) in deionized water is lower than measured in the simulated groundwater systems. The addition of Pb(0) lowered the extent of Sb(0) oxidation due to competitive oxidation or to the coupling of antimony and lead redox reactions. These results can be used to identify substrates that promote precipitation of relatively insoluble antimony compounds in target berm soils and thus prevent the offsite migration of antimony from shooting range target berms.

H.3.5 Cr(VI) Treatment by Zero-Valent Iron

Publication: Julia H. Jamieson-Hanes, Adam M. Lentz, Richard T. Amos, Carol J. Ptacek, David W. Blowes (2014) **Geochim. Cosmochim. Acta** 142, 299-313.

A series of replicate flow-through cell experiments was conducted to characterize Cr isotope fractionation during Cr(VI) treatment by granular zero-valent iron (ZVI). Synthetic groundwater containing 50 mg L^{-1}Cr(VI) was pumped upward through a custom-made cell packed with ZVI under anaerobic conditions. The geochemical evolution of the system was monitored using pH and redox measurements, while aqueous effluent samples were retained for analysis of cations and Cr isotopes. Real-time, in situ X-ray absorption near edge structure (XANES) spectroscopy collected via a Kapton® window in the cell provided additional information on the speciation of the reaction products. Increases in δ^{53}Cr values corresponding to decreases in Cr(VI) concentration suggested the occurrence of redox processes. Spectroscopic results correlated well with the isotope data, indicating reduction of Cr(VI) to Cr(III). The isotope data did not appear to follow a single trend. A two-stage system was proposed to explain the complex isotope trend, where the rapid Cr removal was associated with very little fractionation ($\varepsilon = -0.2$ ‰), whereas slower removal was associated with a greater degree of fractionation ($\varepsilon = -1.2$‰ to -1.5‰). Reactive transport modeling was used to quantify distinct isotope fractionation values (ε), differentiated by a significant change in the Cr removal rate.

H.3.6 Microbial Enhanced Oil Recovery in Fractional-Wet Systems

Publication: Armstrong, R. T., and D. Wildenschild (2012) **Transport Porous Med.** 92 (3), 819-835.

Microbial enhanced oil recovery (MEOR) is a technology that could potentially increase the tertiary recovery of oil from mature oil formations. However, the efficacy of this technology in fractional-wet systems is unknown, and the mechanisms involved in oil mobilization therefore need further investigation. The MEOR strategy investigated here consists of the injection of ex situ produced metabolic byproducts produced by Bacillus mojavensis JF-2 (which lower interfacial tension (IFT) via biosurfactant production) into fractional-wet cores containing residual oil. Two different MEOR flooding solutions were tested; one solution contained both microbes and metabolic byproducts while the other contained only the metabolic byproducts. The columns were imaged with X-ray computed microtomography (CMT) after water flooding, and after MEOR, which allowed for the evaluation of the pore-scale processes taking place during MEOR. Results indicate that the larger residual oil blobs and residual oil held under relatively low capillary pressures were the main fractions recovered during MEOR. Residual oil saturation, interfacial curvatures, and oil blob sizes were measured from the CMT images and used to develop a conceptual model for MEOR in fractional-wet systems. Overall, results indicate that MEOR was effective at recovering oil from fractional-wet systems with reported additional oil recovered (AOR) values between 44 and 80%; the highest AOR values were observed in the most oil-wet system.

H.3.7 Sulfur-Mediated Electron Shuttling During Bacterial Iron Reduction

Publication: Theodore M. Flynn, Edward J. O'Loughlin, Bhoopesh Mishra, Thomas J. DiChristina, Kenneth M. Kemner (2014) **Science** 344, 1039-1042.

Microbial reduction of ferric iron [Fe(III)] is an important biogeochemical process in anoxic aquifers. Depending on groundwater pH, dissimilatory metal-reducing bacteria can also respire alternative electron acceptors to survive, including elemental sulfur (S^0). To understand the interplay of Fe/S cycling under alkaline conditions, we combined thermodynamic geochemical modeling with bioreactor experiments using *Shewanella oneidensis* MR-1. The new 13-ID-E microprobe was used to obtain sulfur K-edge XANES spectra of the S-containing bioreactors to define the sulfur speciation. Under these conditions, *S. oneidensis* can enzymatically reduce S^0 but not goethite (α-FeOOH). The HS^- produced subsequently reduces goethite abiotically. Because of the prevalence of alkaline conditions in many aquifers, Fe(III) reduction may thus proceed via S^0-mediated electron-shuttling pathways.

H.3.8 Uranium in Oxidized Wetland Sediment from the Savannah River Site

Publication: Dien Li, John C. Seaman, Hyun-Shik Chang, Peter R. Jaffe, Paul Koster van Groos, De-Tong Jiang, Ning Chen, Jinru Lin, Zachary Arthur, Yuanming Pan, Kirk G. Scheckel, Matthew Newville, Antonio Lanzirotti, Daniel I. Kaplan (2014) **J. Environ. Radioactiv.** 131, 40-46.

Uranium speciation and retention mechanisms onto Savannah River Site (SRS) wetland sediments was studied using batch (ad)sorption experiments, sequential extraction, U L_3-edge X-ray absorption near-edge structure (XANES) spectroscopy, fluorescence mapping and μ-XANES. Under oxidized conditions, U was highly retained by the SRS wetland sediments. In contrast to other similar but much lower natural organic matter (NOM) sediments, significant sorption of U onto the SRS sediments was observed at pH < 4 and pH > 8. Sequential extraction indicated that the U species were primarily associated with the acid soluble fraction (weak acetic acid

extractable) and organic fraction (Na-pyrophosphate extractable). Uranium L_3-edge XANES spectra of the U-bound sediments were nearly identical to that of uranyl acetate. Based on fluorescence mapping, U and Fe distributions in the sediment were poorly correlated, U was distributed throughout the sample and did not appear as isolated U mineral phases. The primary oxidation state of U in these oxidized sediments was U(VI), and there was little evidence that the high sorptive capacity of the sediments could be ascribed to abiotic or biotic reduction to the less soluble U(IV) species or to secondary mineral formation. Collectively, this study suggests that U may be strongly bound to wetland sediments, not only under reducing conditions by reductive precipitation, but also under oxidizing conditions through NOM-uranium bonding.